Supplementary material for: "Forward and inverse design of single-layer metasurface-based broadband antireflective coating for silicon solar cells"

Anton Ovcharenko[a,*], **Sergey Polevoy**[b], **Oleh Yermakov**[a,c,*]
[a]V. N. Karazin Kharkiv National University, Department of Computational Physics, Kharkiv, Ukraine
[b]O. Ya. Usikov Institute for Radiophysics and Electronics of NAS of Ukraine, Radiospectroscopy Department, Kharkiv, Ukraine
[c]Leibniz Institute of Photonic Technology, Department of Fiber Photonics, Jena, Germany

*Anton Ovcharenko, anton.ovcharenko@karazin.ua; Oleh Yermakov, oe.yermakov@gmail.com

S1 Impact of absorption losses

Here, we present the spatial distributions of the electric and magnetic fields of the TE (970 nm) and TM (870 nm) eigenmodes of the silicon metasurface based on the free-form meta-atoms without silicon substrate at $k_x = 0.95\pi/P$, where P is the period of metasurface (Fig. S3). By adding the silicon substrate, the resonances of the eigenmodes are overlapping in the vicinity of 900 nm. The field distributions have been calculated numerically using the Eigenfrequency Solver of COMSOL Multiphysics.

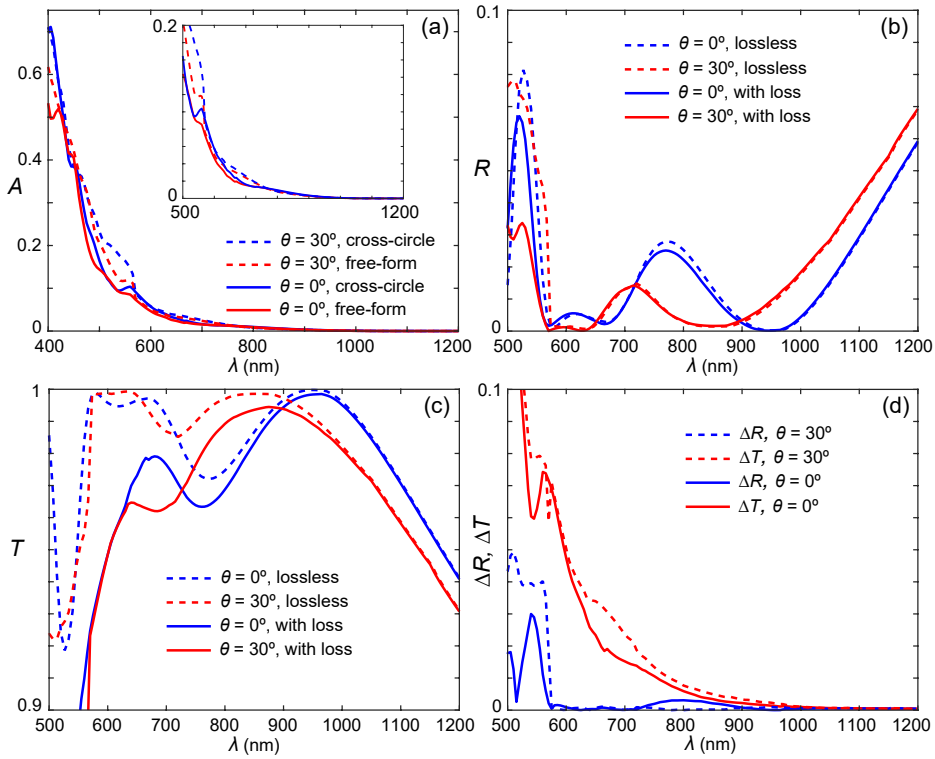

Fig S1 (a-c) Dependencies of the (a) absorptance, (b) reflectance, and (c) transmittance on the wavelength for a dielectric metasurface consisting of the free-form meta-atoms at normal (blue lines) and 30°-oblique (red lines) incidence in the lossless (dashed lines) and lossy (solid lines) cases. (d) The absolute error between the lossless and lossy cases on the wavelength for the reflectance (blue lines) and transmittance (red lines).

S2 Polarization independence

Since our geometries preserve C4 rotation symmetry (an optimization constraint), the optical response is TE/TM polarization independent for normal incident waves [Figs. S2(a)-S2(b)]. Under oblique incidence, the minor difference in TE and TM polarizations emerges [Figs. S2(c)-S2(d)]. The average reflectances for the cross-circle and free-form designs are $\overline{R}_{\mathrm{TE}} = 7.5\%$, $\overline{R}_{\mathrm{TM}} = 4.3\%$ and $\overline{R}_{\mathrm{TE}} = 6.3\%$, $\overline{R}_{\mathrm{TM}} = 4.7\%$, respectively.

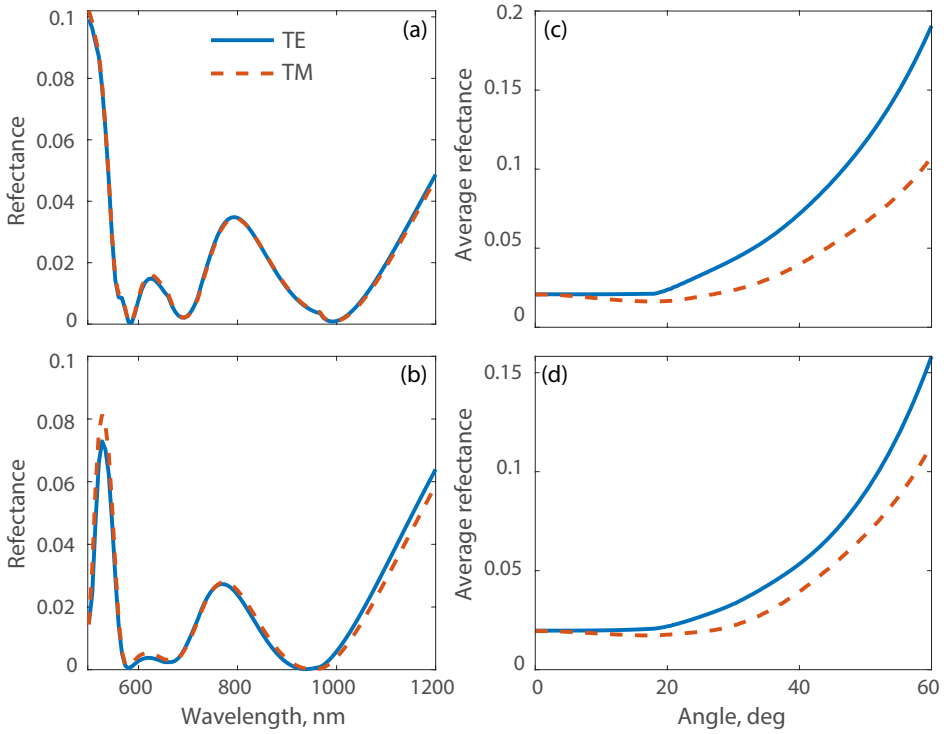

Fig S2 Dependence of the reflectance of TE- (blue solid line) and TM-polarized (red dashed line) on the wavelength for (a,c) cross-circle and (b,d) free-form meta-atoms under (a,b) normal incidence, and (c,d) average over all wavelengths reflectance depending on the incident angle.

S3 TE and TM eigenmodes of dielectric metasurface

Here, we present the spatial distributions of the electric and magnetic fields of the TE (970 nm) and TM (870 nm) eigenmodes of the silicon metasurface based on the free-form meta-atoms without silicon substrate at $k_x = 0.95\pi/P$, where P is the period of metasurface (Fig. S3). By adding the silicon substrate, the resonances of the eigenmodes are overlapping in the vicinity of 900 nm. The field distributions have been calculated numerically using the Eigenfrequency Solver of COMSOL Multiphysics.

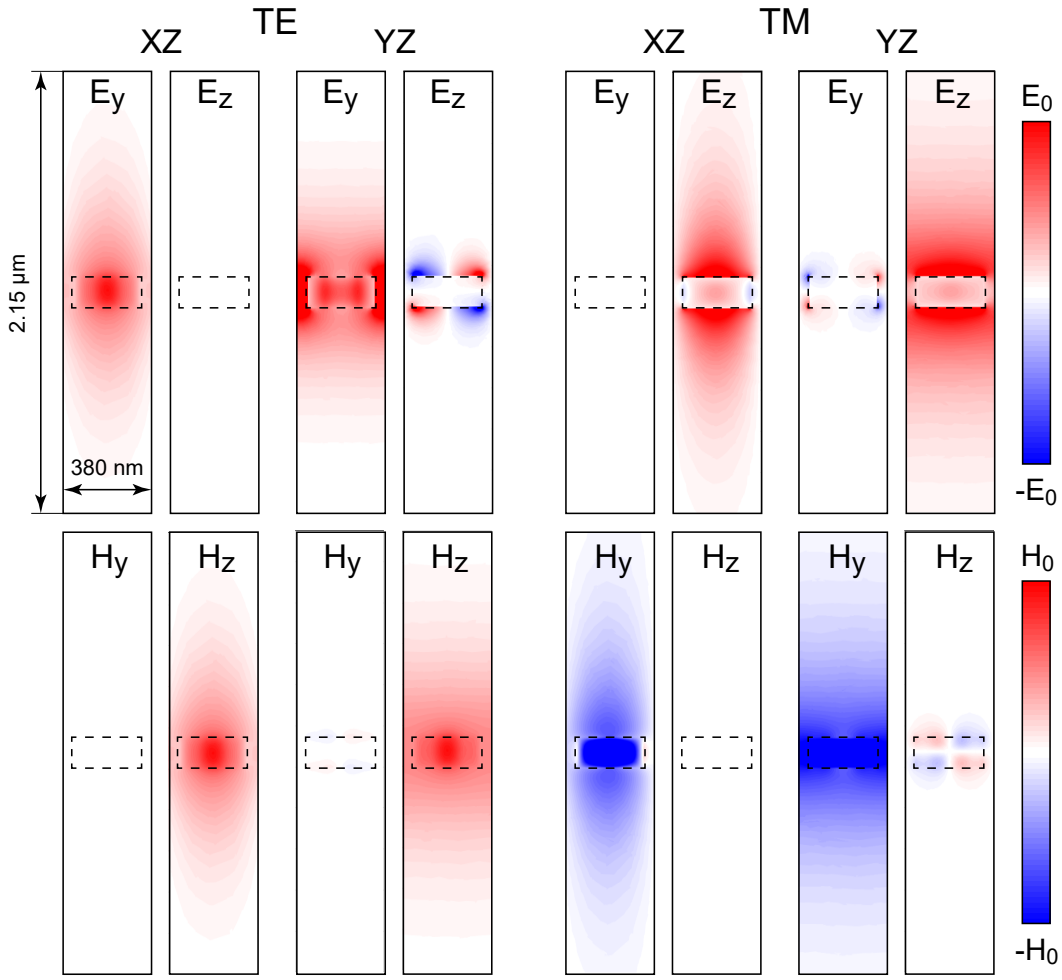

Fig S3 Spatial distribution in the side view of the electric (top row) and magnetic (bottom row) fields in the xz- (first and third columns) and yz-planes (second and fourth columns) for the TE (E_y, H_z) and TM (E_z, H_y) eigenmodes (two left and two right columns, respectively).

S4 Comparison of the numerical simulation methods

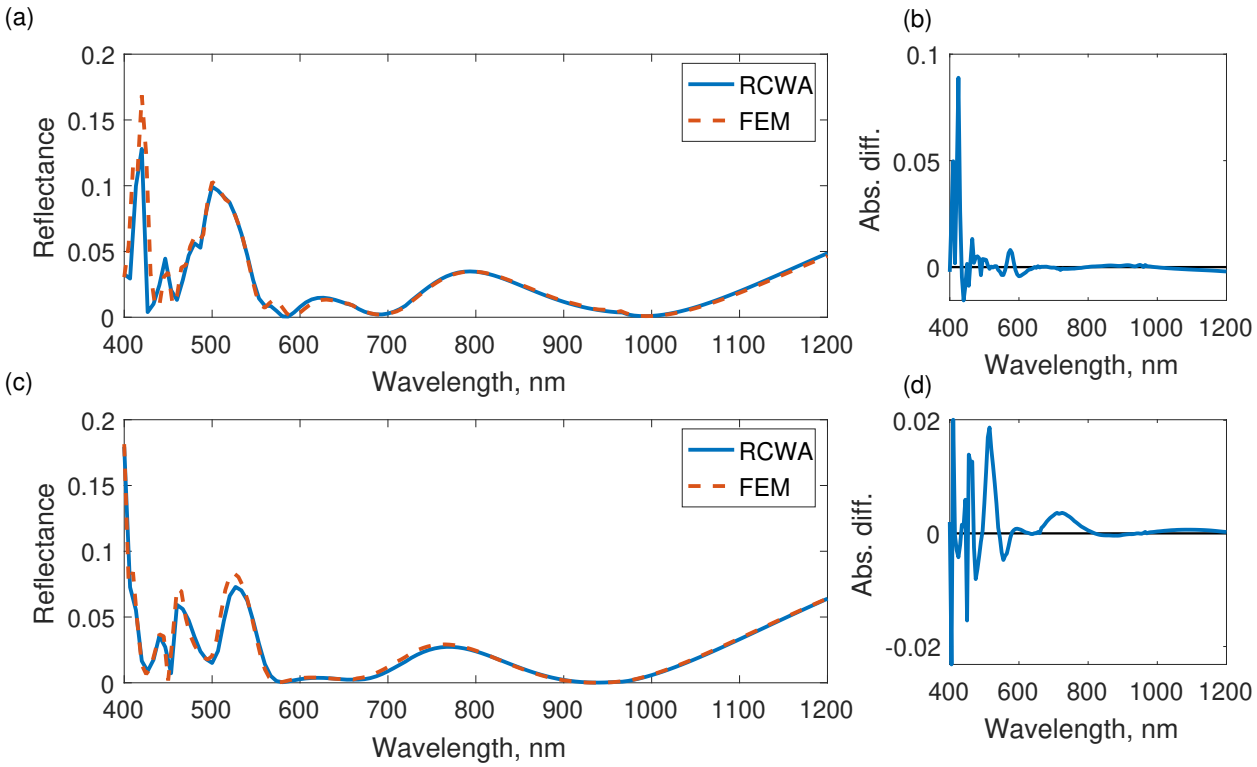

Fig S4 Reflectance spectrum under the normal incidence for (a) cross-circle and (b) free-form meta-atom array calculated with RCWA (blue) and FEM (red) with the maximum cell size of 30 nm. The reflectance values for wavelengths above 600 nm almost completely coincide, while for shorter wavelengths, some differences in reflectance values are observed near the narrow resonances. Subfigures (b) and (d) show absolute differences of the RCWA and FEM reflectance values in (a) and (c), respectively.

S5 GLOnet training process

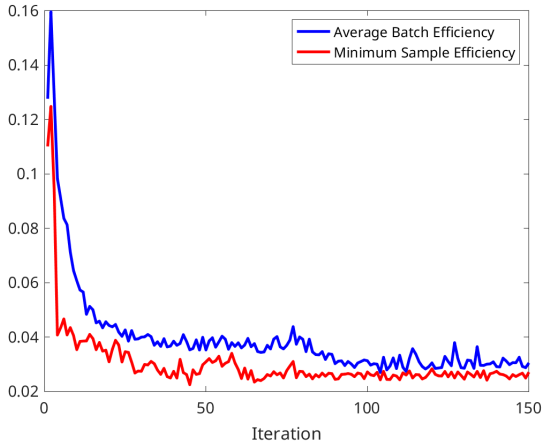

Fig S5 GLOnet optimization progress: loss function values at each iteration. The blue and red lines correspond to the average and minimum values within the batch, respectively.

S6 Field profiles of the cross-circle and free-form meta-atom

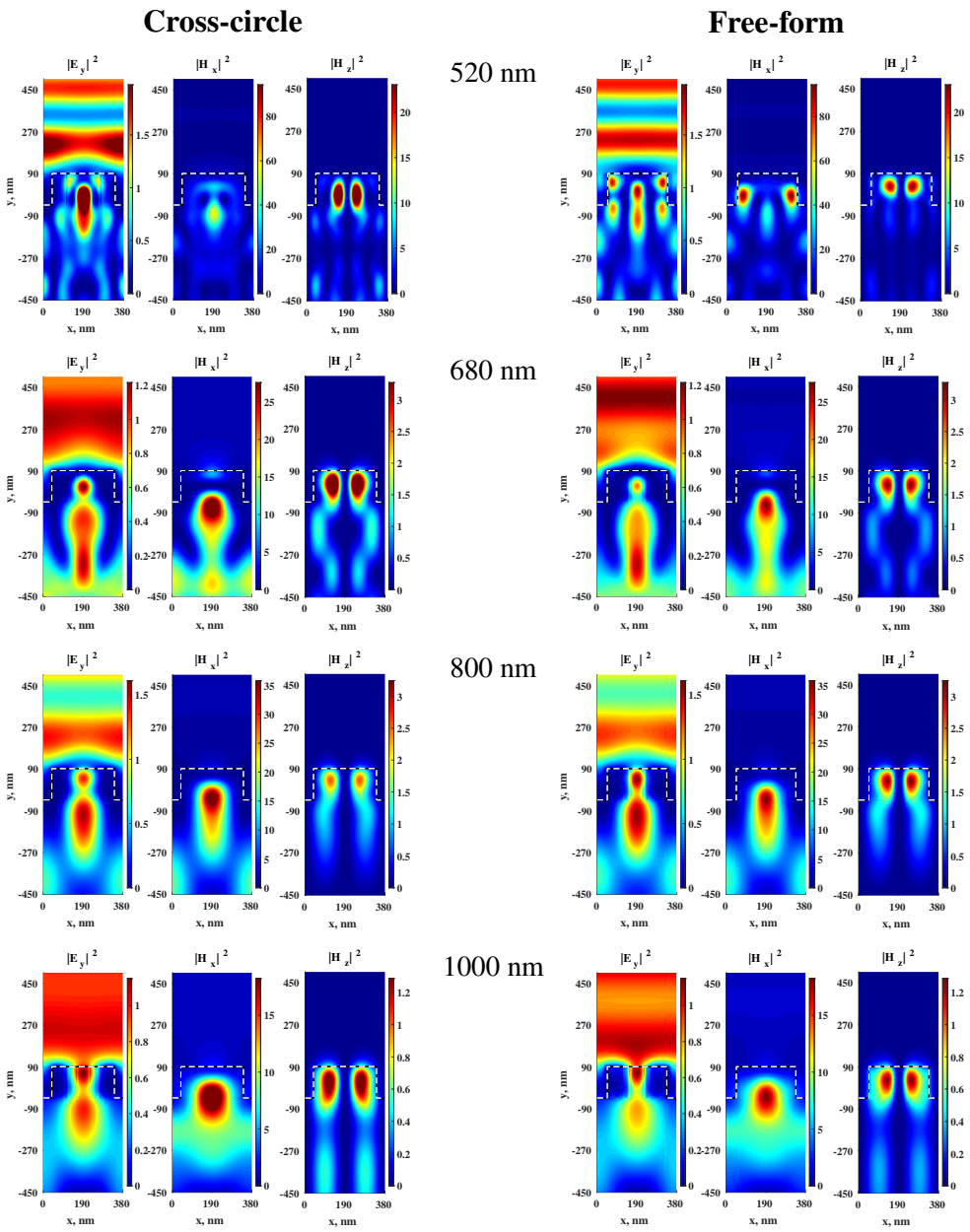

Fig S6 Field profiles at selected wavelengths (labeled in the middle) for the cross-circle (left column) and free-form (right column) designs at the normal incidence.

S7 Local (single-batch) optimization comparison

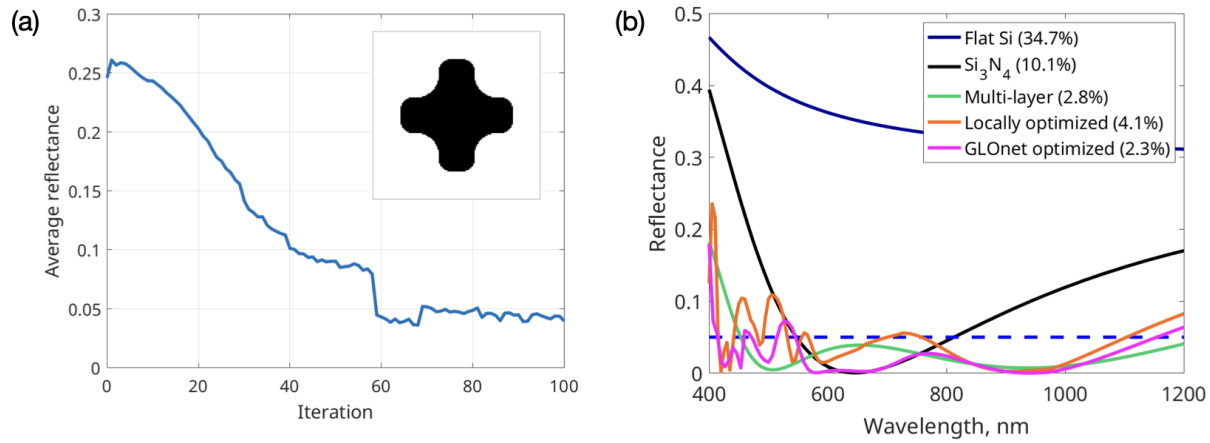

Fig S7 Local optimization of single-layer anti-reflective metasurface. (a) Optimization progress: average reflectance achieved as a function of iterations. The inset shows the best final design achieved after several runs with different random starting points. (b) Comparison of reflectivity with different alternative designs mentioned in the paper. The legend shows average values for each structure.

S8 Details on the designs listed in Table 1 of the main text

Table S1 Key geometric parameters that correspond to the anti-reflection properties listed in Table 1 of the main text for the corresponding designs.

Structure type	Design parameters		
	materials (from top)		thicknesses (nm)
Single-layer uniform coating	Si_3N_4		80
Three-layer thin film stack	MgF_2, SiN, TiO_2		115.2, 47.6, 36.7
	period (nm)	height/coating (nm)	size parameter (nm)
Coated silicon cylinders	475	150/80	diameter: 375
Silicon cylinders	450	150/0	diameter: 288
Dual-sized pillars	400	140/0	square sides: 110 & 185 nm
Cross-circle waveguide	380	150/0	R: 90, W: 60, L: 300